ARTICLES
https://doi.org/10.1038/s41929-021-00643-9
nature catalysis

Check for updates

Stereodefined rhodium-catalysed 1,4-H/D delivery for modular syntheses and deuterium integration

Weiyi Wang[1,4], Yibo Yu[1,4], Bao Cheng[1], Huayi Fang[2], Xue Zhang[3] ✉, Hui Qian[1] ✉ and Shengming Ma[1,3] ✉

Deuterium-incorporated compounds are of high interest owing to their importance in the pharmaceutical industry, organic synthesis and materials science. So far, the integration of deuterium into the inert, saturated magic methyl or methylene groups of covalent molecules remains challenging. Here, we present a 1,4-H delivery of allylic metallic species to provide a highly stereoselective and straightforward approach to 3-methyl-2(*E*)-enals or -enones from readily available 2,3-allenols and organoboronic acids. The reaction accommodates many synthetically versatile functional groups as well as multi-pharmacophores, and is not limited to the formation of 3-methyl derivatives. By applying 1,4-H or D delivery, deuterium atom(s) from differently deuterated allenols can be edited into the methyl or methylene groups of versatile organic skeletons, resulting in the efficient formation of 4-monodeuterated, 1,4- and 4,4-doubly deuterated, and 4,4,4-triply deuterated 2(*E*)-enals or -enones. These powerful platform molecules can provide straightforward paths to other deuterated compounds for different purposes.

Deuteration is essential and is widely used in the pharmaceutical industry[1–3], organic synthesis[4,5] and materials science[6–8]. In drug discovery, deuteration has great potential to improve the pharmacological profiles of lead compounds or to enable the tracing of metabolic pathways to elucidate a drug's mechanism of action[1–3] (Fig. 1a). On the other hand, the magic methyl effect has been extensively observed in natural products[9,10] and in medicinal chemistry[11–18] (Fig. 1a,b). For example, the incorporation of a methyl group into certain lead compounds can dramatically boost their potency[15] (Fig. 1b, bottom). Thus, due to the corresponding effects of deuterium atoms on the absorption, distribution, metabolism and excretion[3,19] of compounds, the robust generation of CH_nD_{3-n} ($n = 0$, 1, 2) groups in covalent molecules is of high current interest. So far, the modular creation of differently deuterated methyl and methylene groups in covalent molecules remains a fundamental challenge[20–28] (Fig. 1a). Organic transition metal species are involved in catalytic reactions[29–31] and are prevalent in medicinal chemistry[14,32] and materials science[33,34]. In a β-H elimination reaction, the metal picks up a hydrogen atom in an alkyl metallic species. The frequently used **A**-type allylic metallic species may also undergo this type of β-H elimination to afford 1,3-dienes, in which intermediate **B**[35–37] is generated during the process of obtaining the hydrogen atom (Fig. 1c, path a and path b). We envisioned that the hydrometallation of the $C^3{=}C^4$ bond instead of the $C^1{=}C^2$ bond in intermediate **B** would yield an isomeric allylic intermediate **C** (Fig. 1c, path c), formulating a concept for allylic C–H activation[38–47] that eventually results in a metal-carried 1,4-H delivery. Challenges involve control of the regioselectivity in terms of the two C=C bonds in intermediate **B**, and the realization of clear-cut, one-way transformation.

Here we report a reaction of organoboronic acids with 2,3-allenols, co-catalysed by Rh and Cu and using air to complete the catalytic cycle, which affords synthetically and/or medicinally versatile 2-alkenals or 2-alkenones with an excellent stereoselectivity under very mild conditions (Fig. 1d, left). By applying this protocol, a deuterium atom is edited into the methyl or the methylene groups of versatile organic skeletons via its robust delivery from the C(D)OH moiety of differently deuterated, readily available allenols (Fig. 1d, right).

Results

Reaction discovery and optimization. Carbometallation of allenes has become one of the most common approaches for the facile formation of **A**-type allylic metallic species[48,49]. We therefore attempted the Rh-catalysed reaction of 2,3-butadienol **1a** with 3-methoxyphenyl boronic acid **2a** to test the concept shown in Fig. 1c, under the same conditions as for the *syn*-hydroarylation of propargylic alcohols[50]. Different from the expected hydroarylation reaction[50], a new product, 3-(*m*-methoxyphenyl)but-2(*E*)-enal *E*-**3aa**, was formed in a highly stereoselective manner, albeit in 12% NMR yield (Table 1, entry 1). Through careful analysis of its structure, we noticed that the carbon atom in the 4-position may indeed have received a hydrogen atom from the carbon atom in the 1-position of **1a** during this transformation. After further optimization, we observed that 2-enal *E*-**3aa** could be formed in 77% NMR yield in the presence of $[Cp^*RhCl_2]_2$ (where Cp^* is pentamethylcyclopentadienyl) (2.5 mol%), $Cu(OAc)_2{\cdot}H_2O$ (1.2 equiv.) and NaOAc (20 mol%) in MeOH at room temperature in air (entry 2). Solvent screening showed that tetrahydrofuran (THF) was optimal (entries 2–7). A 90% NMR yield of *E*-**3aa** was observed when the reaction was conducted with 1.0 equiv. of $Cu(OAc)_2{\cdot}H_2O$ (entry 8); however, it could also be used in catalytic amounts (entries 9 and 10). The efficiency decreased when the reaction was carried out in the

[1]Research Center for Molecular Recognition and Synthesis, Department of Chemistry, Fudan University, Shanghai, P. R. China. [2]Department of Chemistry, Fudan University, Shanghai, P. R. China. [3]State Key Laboratory of Organometallic Chemistry, Shanghai Institute of Organic Chemistry, Chinese Academy of Sciences, Shanghai, P. R. China. [4]These authors contributed equally: Weiyi Wang, Yibo Yu. ✉e-mail: xzhang@sioc.ac.cn; qian_hui@fudan.edu.cn; masm@sioc.ac.cn

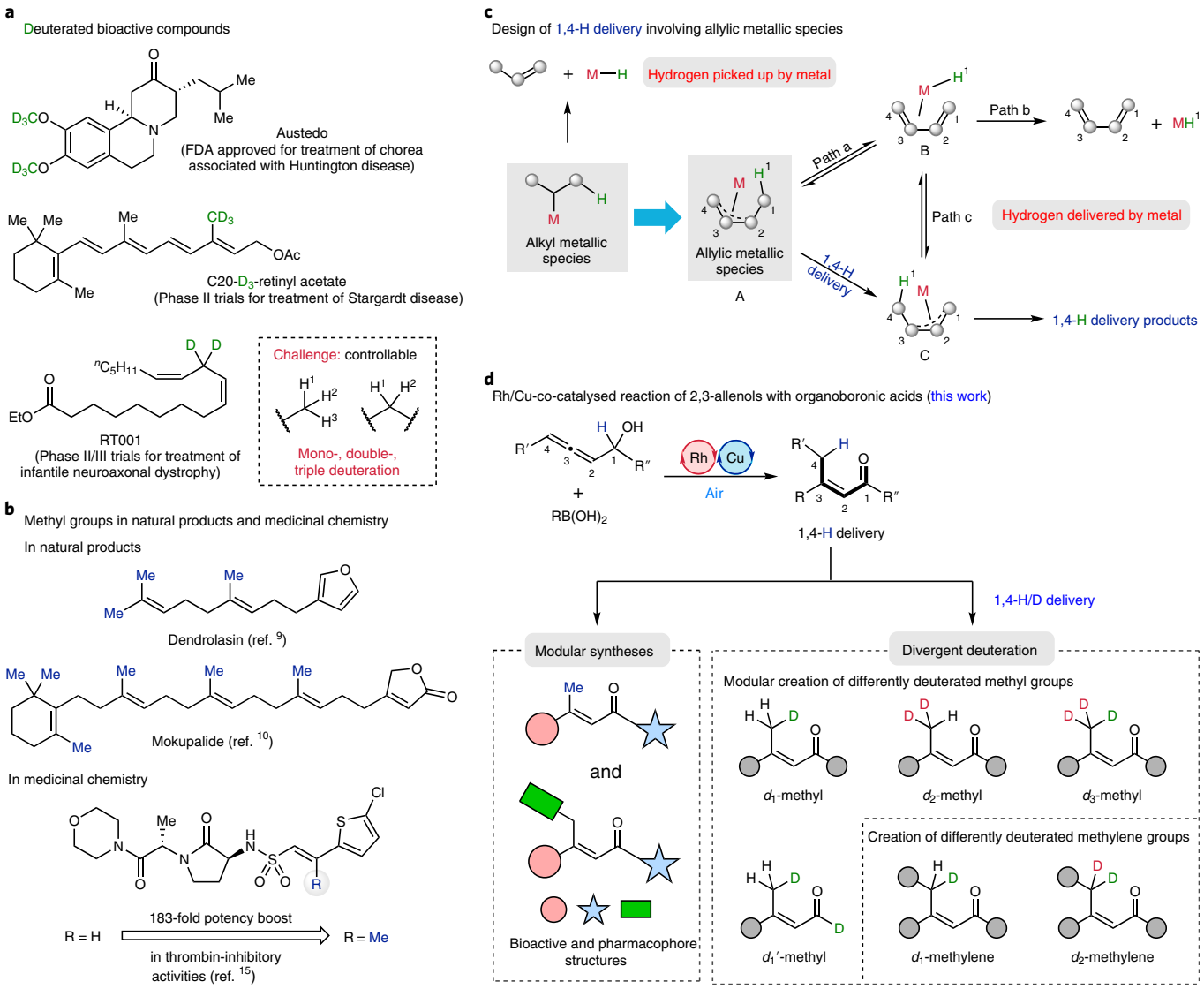

Fig. 1 | The importance of deuterated compounds, the magic methyl effect and strategies for deuteration. a, Selected examples of deuterated bioactive compounds. FDA, United States Food and Drug Administration. **b**, Methyl groups in natural products (top) and medicinal chemistry (bottom). **c**, The concept of 1,4-H delivery. **d**, Rh/Cu-co-catalysed reaction of 2,3-allenols with organoboronic acids involving 1,4-H/D delivery.

absence of NaOAc (entry 11), and an NMR yield of only 4% *E*-**3aa** was obtained in the absence of $Cu(OAc)_2{\cdot}H_2O$ (entry 12), indicating the critical roles of the acetate anion and the Cu salt. Further evaluation of other Rh catalysts indicated that neither Rh(I) nor Rh(II) catalysts could catalyse this transformation (entries 13–16).

Substrate scope and applications. With the optimized conditions (Table 1, entry 10) in hand, we next examined the substrate scope for the generation of 3-methyl-substituted products (Fig. 2a). It is noteworthy that, in all cases, an excellent *E*-stereoselectivity was achieved without affording the *Z*-isomers. At first, a variety of commercially available arylboronic acids bearing different substituents were reacted with 2,3-butadienol **1a** (Fig. 2a, top). Both electron-rich and electron-deficient arylboronic acids reacted to afford the corresponding products (*E*-**3aa** to *E*-**3ar**) in high yields, with the more electron-rich arylboronic acids giving the higher yields. Importantly, a variety of synthetically useful functional groups—including methoxy (*E*-**3aa** and *E*-**3ad**), bromo (*E*-**3ae** and *E*-**3af**), chloro (*E*-**3ag**), fluoro (*E*-**3ah**), trifluoromethyl (*E*-**3ai**), acetyl (*E*-**3aj**), methoxycarbonyl (*E*-**3ak**), cyano (*E*-**3al**) and nitro (*E*-**3am**)—were tolerated. 2-Naphthyl and heteroaryl groups such as thienyl and furyl can also be incorporated in the products with decent yields (*E*-**3ao** to *E*-**3ar**). The loading of $[Cp^*RhCl_2]_2$ could be reduced to 1.0 mol% (*E*-**3aa**, *E*-**3ac**, *E*-**3ad**, *E*-**3ae**, and *E*-**3al**). X-ray crystallography analysis of *E*-**3ak** further confirmed the structure of the product and its stereochemistry. In addition to primary allenols, secondary allenols also worked well under the standard conditions, affording corresponding 2(*E*)-enones in high yields (Fig. 2a, bottom). Notably, we found that the scope of boronic acids was not limited to arylboronic acids: an alkenylboronic acid also gave the desired 2,4-dienone product (*E*,*E*)-**3du**, and even alkylboronic acids could be employed to afford the corresponding ketones with good yields (*E*-**3cv**, *E*-**3iv** and **3dw**). The structure and stereochemistry of the 2(*E*)-enone products were further confirmed by the single-crystal X-ray diffraction analysis of *E*-**3ed**. Gram-scale reaction of allenol **1f** with boronic acid **2d** afforded a 76% yield of the desired product *E*-**3fd** as single isomer under the standard conditions. The reaction is not limited to the syntheses of 3-methyl-substituted products; 4-aryl or alkyl-substituted 2,3-allenols were also successful in this transformation, affording

Table 1 | Optimization of the reaction conditions

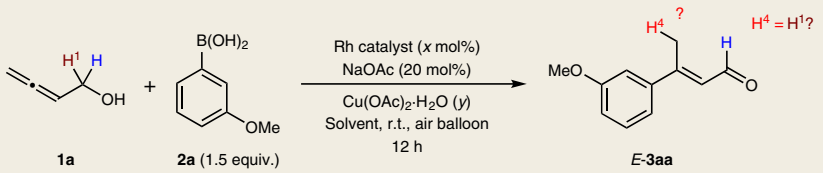

1a 2a (1.5 equiv.) E-3aa

Entry	Rh catalyst	x	y	Solvent	NMR yield[a] (%)
1[b]	$[Cp^*RhCl_2]_2$	2.5	0	MeOH	12
2	$[Cp^*RhCl_2]_2$	2.5	1.2 equiv.	MeOH	77
3	$[Cp^*RhCl_2]_2$	2.5	1.2 equiv.	Dioxane	79
4	$[Cp^*RhCl_2]_2$	2.5	1.2 equiv.	Toluene	75
5	$[Cp^*RhCl_2]_2$	2.5	1.2 equiv.	THF	86
6	$[Cp^*RhCl_2]_2$	2.5	1.2 equiv.	MeCN	81
7	$[Cp^*RhCl_2]_2$	2.5	1.2 equiv.	Dichloromethane	51
8	$[Cp^*RhCl_2]_2$	2.5	1.0 equiv.	THF	90
9	$[Cp^*RhCl_2]_2$	2.5	20 mol%	THF	85
10	$[Cp^*RhCl_2]_2$	2.5	5 mol%	THF	86
11[c]	$[Cp^*RhCl_2]_2$	2.5	5 mol%	THF	62
12	$[Cp^*RhCl_2]_2$	2.5	0	THF	4
13	$Rh(PPh_3)_3Cl$	5	5 mol%	THF	0
14	$[Rh(cod)Cl]_2$	2.5	5 mol%	THF	2
15	$[Rh(C_2H_4)_2Cl]_2$	2.5	5 mol%	THF	1
16	$[Rh(OAc)_2]_2$	2.5	5 mol%	THF	0
17	$RhCl_3$	5	5 mol%	THF	0

The reaction was conducted with 0.5 mmol **1a**, 0.75 mmol **2a**, *x* mol% Rh catalyst, 20 mol% NaOAc and *y* equivalents or mol% $Cu(OAc)_2·H_2O$ in 2.5 ml solvent at room temperature for 12 h with an air balloon. [a]The yield was determined by ^1H NMR analysis using dibromomethane as the internal standard. [b]The reaction was conducted with 15 mol% $AgBF_4$ under argon for 4 h. [c]The reaction was conducted without NaOAc.

the desired 3-non-methyl-substituted products *E*-**3ka**, *E*-**3lo**, *E*-**3mb**, *E*-**3nx** and *E*-**3od** in 53–70% yields (Fig. 2b).

Because α,β-unsaturated enals and enones are versatile building blocks in organic synthesis, such products have a wide range of synthetic applications (for details, see Supplementary Fig. 3). The 2-enal *E*-**3ad** could undergo 1,2-addition with EtMgBr, a condensation reaction with ethyl acetate in the presence of lithium diisopropylamide, and a Wittig reaction to afford the corresponding allyl alcohols *E*-**4** (86% yield) and *E*-**5** (91% yield) and the 1,3-diene (*E*,*E*)-**6** (85% yield). The α,β-unsaturated enone *E*-**3fd** could undergo Suzuki coupling and reduction with $NaBH_4$ to afford *E*-**7** (86% yield) and *E*-**8fd** (91% yield) in high yields.

The α,β-unsaturated carbonyl motif in these products is one of the common warheads of targeted covalent inhibitors[51–53]. Here we further demonstrate the scope of this reaction via the incorporation of molecular units with potential bioactivity into the enals or enones (Fig. 3). By applying sequential alkynylation, an allenation of terminal alkyne (ATA) reaction[54] and the current reaction, a variety of structurally complex molecules were modified using three different strategies. First, the alkynylation of structurally complex aldehydes followed by an ATA reaction afforded terminal allenols (**1j** and **1p**) or 3-substituted allenols (**1q** and **1r**), which reacted with various organoboronic acids to afford corresponding unsaturated aldehyde compounds (*E*-**3qd** and *E*-**3rd**) and ketones ((*S*)-*E*-**3jt** and *E*-**3pe**) (Fig. 3a). Second, structurally complex molecules with biological activity—such as estrone and glycyrrhetinic acid—were easily incorporated into the organoboronic acids (**2y** and **2z**), enabling the syntheses of corresponding unsaturated aldehydes (*E*-**3ay** and *E*-**3az**) by their reactions with 2,3-butadienol **1a** (Fig. 3b). Third, this strategy was used to assemble multiple structurally complex, biologically active molecular units into one single, more complex molecule (Fig. 3c). For example, diacetone-D-glucose and lithocholic acid could be efficiently incorporated into *E*-**3saa** with 80% yield. Finally, *E*-**3uy**—which contains bioactive units from adapalene, estrone and lithocholic acid—was successfully constructed.

Mechanistic investigation and divergent deuteration. To elucidate the mechanism, the reaction was carried out using allenol **1v**-d_1, which contains a deuterium atom at the α-position of the hydroxyl group. This reaction afforded *E*-**3vd**-d_1 in 86% yield with 99% deuterium incorporation at the allylic position (Fig. 4a), confirming the 1,4-D delivery concept shown in Fig. 1c. This 1,4-D delivery was further optimized to develop a controllable method for precise deuterium incorporation into methyl and methylene groups (Fig. 4b): the ATA reaction of deuterated propargylic alcohols (**PA**-d_1 and **PA**-d_2) and non-deuterated paraformaldehyde afforded α-deuterated allenols (**1**-d_1 and **1**-d_2'), which reacted with organoboronic acids under the standard conditions to afford the corresponding β-monodeuterated methyl 2(*E*)-enones (d_1-methyl products) or 1,4-doubly deuterated 2(*E*)-enals (d_1'-methyl products). Similarly, starting from non-deuterated propargylic alcohols (**PA**) and fully deuterated paraformaldehyde, d_2-methyl products (*E*-**3**-d_2) were afforded. β-Trideuterated methyl enones (d_3-methyl products) were also afforded from deuterated propargylic alcohols (**PA**-d_1) and deuterated paraformaldehyde. The d_3-methyl group could also be successfully incorporated into the structurally complex and potentially bioactive molecules *E*-**3iy**-d_3 and *E*-**3daa**-d_3.

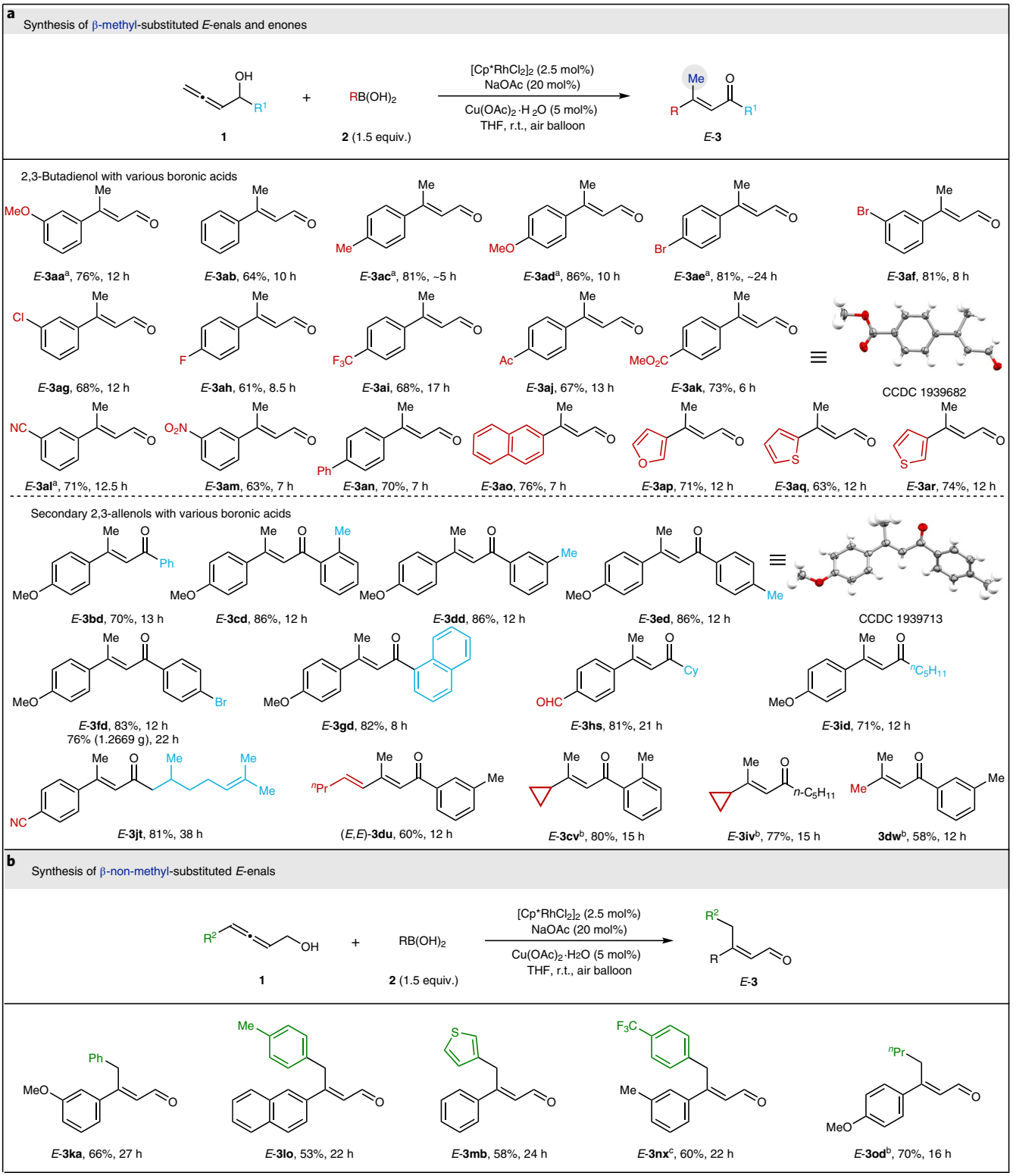

Fig. 2 | Scope of the reaction of allenols 1 with organoboronic acids 2. The reaction was conducted with 1.0 mmol **1**, 1.5 mmol **2**, 2.5 mol% $[Cp^*RhCl_2]_2$, 20 mol% NaOAc and 5 mol% $Cu(OAc)_2{\cdot}H_2O$ in 5 ml THF at room temperature (r.t.) with a balloon of air. **a**, Synthesis of β-methyl-substituted *E*-enals (top) and enones (bottom). **b**, Synthesis of β-non-methyl-substituted *E*-enals. [a]1.0 mol% $[Cp^*RhCl_2]_2$ was used. [b]The reaction was carried out at 50 °C. [c]The yield was determined by ^1H NMR analysis using dibromomethane as the internal standard. The aldehyde was not stable during the isolation. We characterized the corresponding alcohol after reduction with $NaBH_4$.

Furthermore, this powerful approach could also realize controllable deuteration of the methylene group, as shown in the syntheses of *E*-**3wa**-d_1 and *E*-**3wa**-d_2.

To further disclose the mechanism, we performed reactions with allenol **1f** (Fig. 5a, reaction 1) and allyl alcohol *E*-**8fd** (Fig. 5a, reaction 2) under the standard conditions. Both reactions failed to

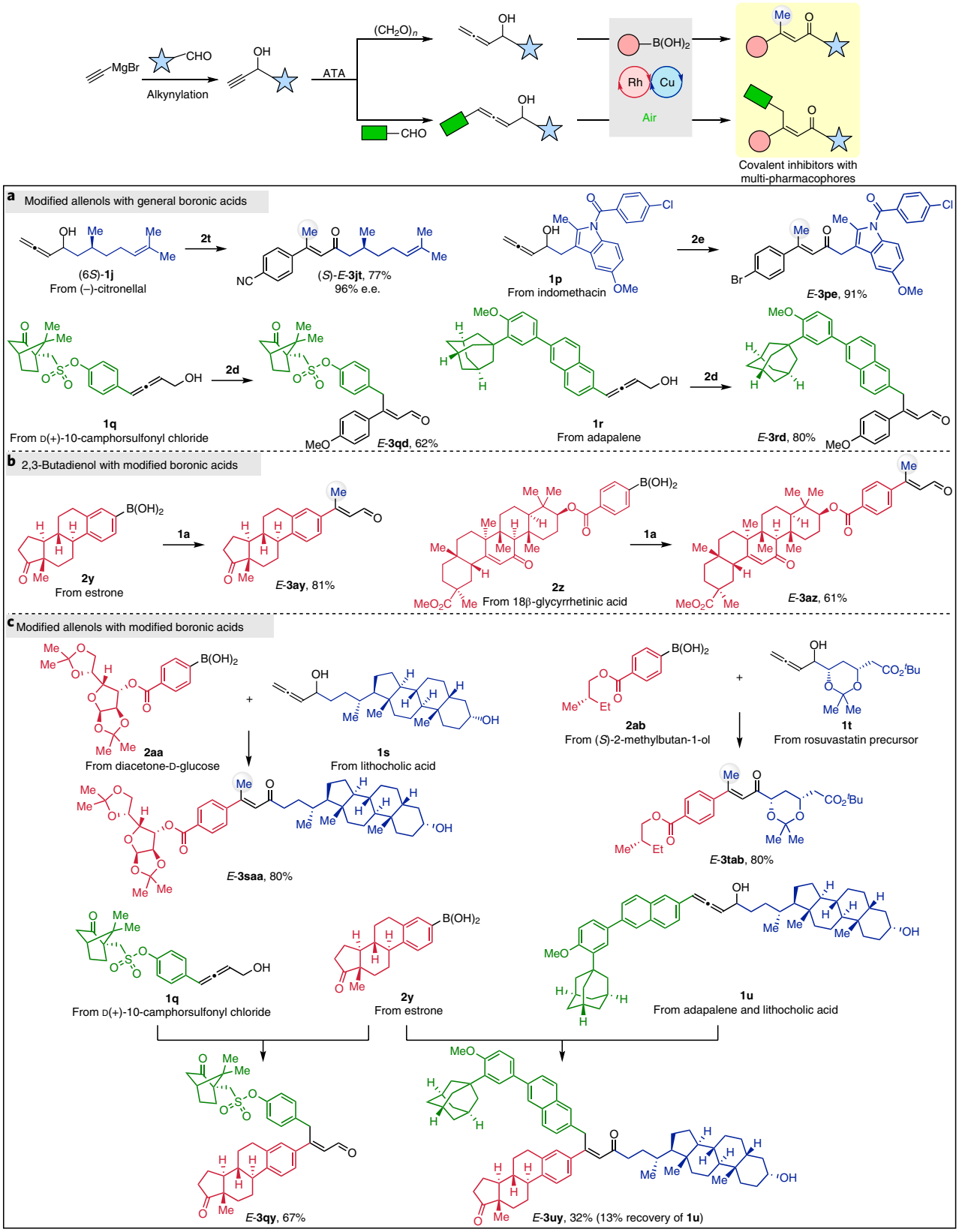

Fig. 3 | Modular incorporation of pharmacophores. a, Reaction of modified allenols with general boronic acids. **b**, Reaction of 2,3-butadienol with modified boronic acids. **c**, Reaction of modified allenols with modified boronic acids.

afford the related ketones **9** and *E*-**3fd**, which excludes the possibility of **9** and *E*-**8fd** as intermediates. Thus, the mechanism involving rhodium alkoxide intermediates **B′1** and **B′2**—which occurs in the Rh-catalysed isomerization of allylic alcohol[55–57]—can be excluded. We determined the kinetic isotope effect to be approximately 1.0 (Fig. 5b), which demonstrated that the C–H bond cleavage was

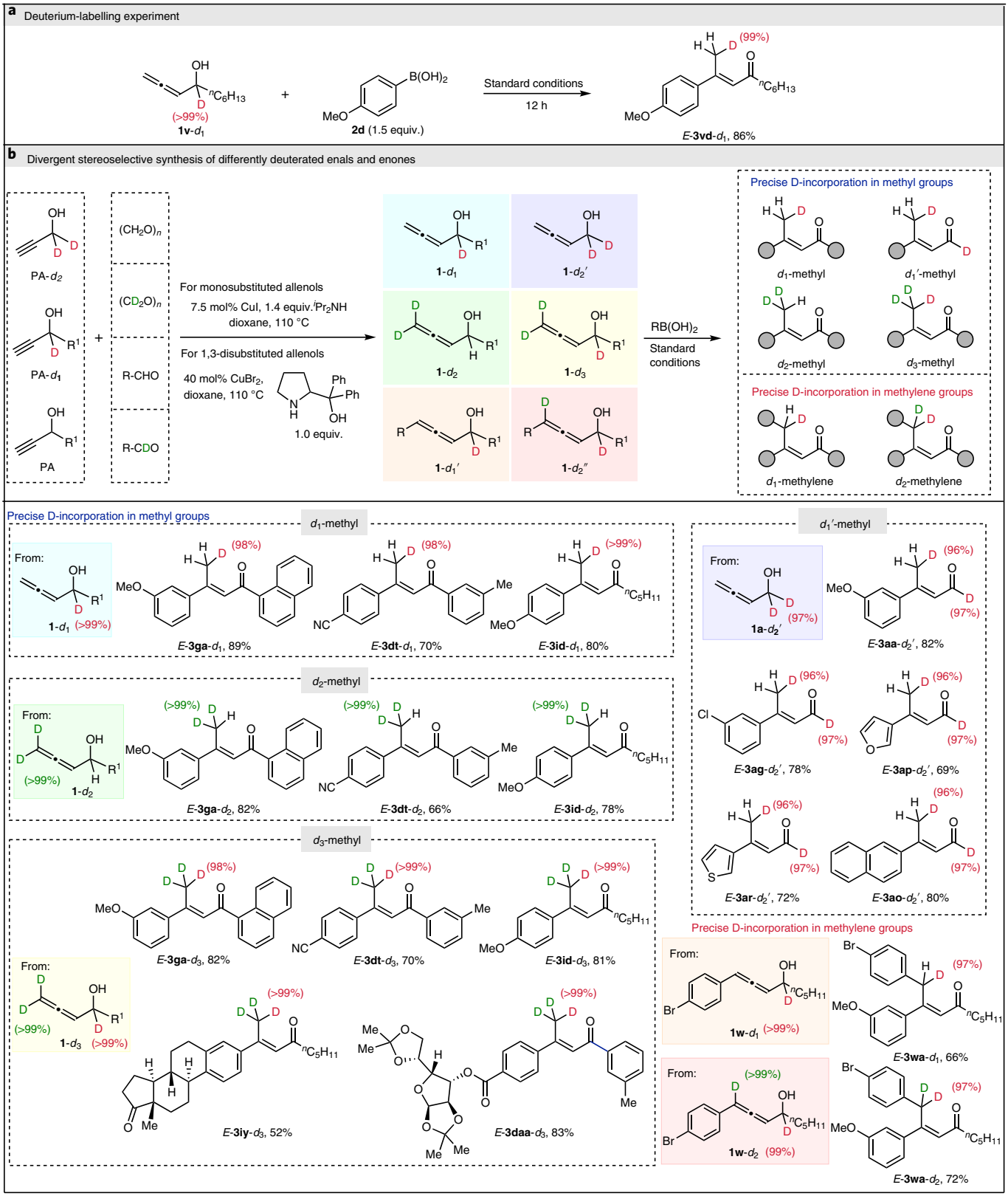

Fig. 4 | Divergent syntheses of deuterated compounds. Standard conditions: 1 equiv. **1**, 1.5 equiv. **2**, 2.5 mol% $[Cp^*RhCl_2]_2$, 20 mol% NaOAc and 5 mol% $Cu(OAc)_2{\cdot}H_2O$ in THF at r.t. with a balloon of air. **a**, Deuterium labelling experiment. **b**, Divergent syntheses of differently deuterated enals and enones.

not the rate-determining step. To pursue a further understanding of the mechanism, we performed density functional theory calculations at the M06/6-311+G(d,p)-SDD/IEFPCM(THF)//M06/6-31G(d)-LANL2DZ level of theory to investigate the reaction energy profiles, using 2,3-butadienol **1a** and phenyl boronic acid **2b** as the model substrates (for more detailed information, see Supplementary

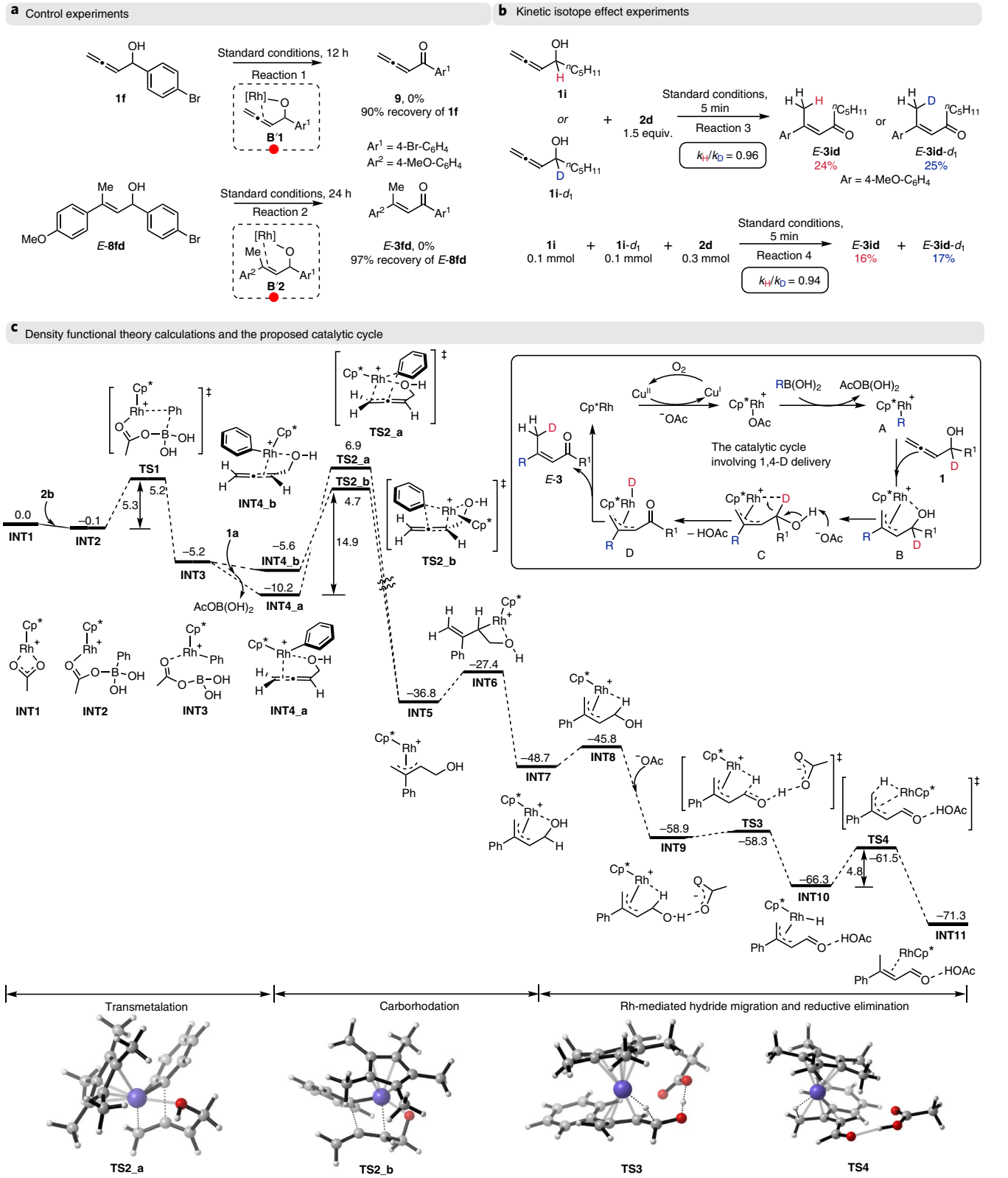

Fig. 5 | Mechanistic studies. Standard conditions: 1 equiv. **1**, 1.5 equiv. **2**, 2.5 mol% $[Cp^*RhCl_2]_2$, 20 mol% NaOAc and 5 mol% $Cu(OAc)_2{\cdot}H_2O$ in THF at r.t. with a balloon of air. **a**, Control experiments. **b**, Kinetic isotope effect experiments. k_H is the rate of the reaction associated with **1i**; k_D is the rate of the reaction associated with **1i**-d_1. **c**, Density functional theory calculations at the M06/6-311+G(d,p)-SDD/IEFPCM(THF)//M06/6-31G(d)-LANL2DZ level of theory, and the proposed catalytic cycle. Free energies are given in kcal mol^{-1} with respect to **INT1**.

Methods). The Gibbs energies incorporate the solvent effect of THF. As shown in Fig. 5c, the transmetallation of $[Cp^*RhOAc]^+$ **INT1** with **2b** proceeds via **TS1**, which requires an activation energy of 5.3 kcal mol^{-1}, resulting in the formation of **INT3**. The subsequent dissociation of $B(OAc)(OH)_2$ and the coordination of the allene moiety of **1a** provides the metal-η^2-allene intermediates: both C=C

bonds of 2,3-butadienol **1a** could coordinate with the Rh(III) centre to generate the intermediates **INT4_a** or **INT4_b**, in which the hydroxyl group also coordinates to the Rh(III) centre. **INT4_a** is found to be lower in free energy than **INT4_b** by 4.6 kcal mol^{-1}. The subsequent insertion of the coordinated allenic C=C double bond into the Rh–C bond via **TS2_a** or **TS2_b** would provide the same π-allyl Rh(III) complex **INT5**, which could easily isomerize to a more stable π-allyl Rh(III) complex **INT7**, with the coordination of the hydroxyl group occurring via the intermediate σ-allyl Rh(III) complex **INT6**. Moreover, the transition structure **TS2_a**, which is associated with the more stable precursor **INT4_a**, is calculated to be less favourable than **TS2_b** by 2.2 kcal mol^{-1} (6.9 versus 4.7 kcal mol^{-1}) due to the existence of steric hindrance between the hydroxyl and the phenyl group in **TS2_a**. Notably, the coordination of the hydroxyl group with the Rh(III) centre stabilizes the π-allyl Rh(III) complex **INT7** by 11.9 kcal mol^{-1} compared with the kinetically favourable intermediate **INT5**. Subsequent isomerization of **INT7** afforded the precursor for the hydride transfer, **INT8**, in which the coordination of the hydroxyl group to the Rh(III) centre is replaced by an agostic interaction between the metal and the hydrogen atom. A hydrogen bond formed between the hydroxyl group of **INT8** and an acetate anion leads to the generation of complex **INT9**, which is exergonic by 13.1 kcal mol^{-1} (relative to **INT8**). Subsequent hydride migration is realized with the assistance of the acetate and proceeds through a concerted transition state **TS3**, in which the acetate anion acts as a base to deprotonate the hydroxylic hydrogen while the coordinated hydrogen migrates to the Rh(III) centre. This hydride-transfer step is exergonic (with an exergonicity of 7.4 kcal mol^{-1}) and requires an activation barrier of only 0.6 kcal mol^{-1} (**TS3**), affording the Rh(III) hydride complex **INT10**. Subsequently, the reductive-elimination step—which involves the migration of the hydride ligand to the terminal allylic carbon and the simultaneous coordination of the reductive Rh(I) centre to the C=C bond of the final 2-alkenal product ***E*-3ab**—needs to overcome a free-energy barrier of 4.8 kcal mol^{-1} (**TS4**). Finally, the oxidation of Rh(I) with Cu in air regenerates the Rh(III) catalyst to complete the catalytic cycle. Overall, the carborhodation step features the highest free-energy barrier of the whole process (14.9 kcal mol^{-1}, **TS2_b**), and is therefore most likely to be the rate-limiting step. It is noteworthy that the Rh(III) centre readily acts as a shuttle in the hydrogen relay to facilitate the 1,4-hydride transfer process (from **INT9** to **INT11**), making it both thermodynamically and kinetically favourable and therefore not the rate-determining step; this is confirmed by the data shown in Fig. 5b.

On the basis of these data, we propose a catalytic cycle (Fig. 5c, top right) that is different from the original concept shown in Fig. 1c. At first, [Cp*RhOAc]$^+$ undergoes transmetallation with the organoboronic acid to generate [Cp*RhR]$^+$ species **A**. Subsequent *syn*-insertion and allylic Rh coordination with OH result in the exclusive formation of the stereodefined allylic rhodium intermediate **C**, in which the hydride participates in an agostic interaction with the Rh through further rotation about the C–C single bond. Subsequent deprotonation of the hydroxyl group and β-D elimination mediated by OAc$^-$ leads to the formation of allylic Rh species **D**, which results in the formation of the product *E*-**3** and Cp*Rh species via reductive elimination. The catalytically active species [Cp*RhOAc]$^+$ can be regenerated via the oxidation of Cp*Rh species using oxygen from air and acetate anion under Cu catalysis, to complete the catalytic cycle.

Conclusions

In conclusion, the concept of metal-carried 1,4-H delivery of allylic metallic species has been developed and applied for the highly stereoselective syntheses of *E*-enals and enones from widely available organoboronic acids and 2,3-allenols under very mild reaction conditions. The reaction has a very broad substrate scope, tolerating many functional groups as well as pharmacophores, and—via the corresponding 1,4-H or D delivery—provides a controllable strategy for the precise incorporation of deuterium into the methyl and methylene groups of covalent molecules from differently deuterated 2,3-allenols. The reaction is co-catalysed by $[Cp^*RhCl_2]_2$ and $Cu(OAc)_2$, with the assistance of oxygen from air to complete the catalytic cycle. Further studies, including investigation of the potential bioactivity of the products and further synthetic applications, are currently ongoing in our laboratory.

Methods

General procedure for the synthesis of enals or enones 3. To a Schlenk flask we added $[Cp^*RhCl_2]_2$ (15.5 mg, 0.025 mmol), NaOAc (16.4 mg, 0.20 mmol), $Cu(OAc)_2{\cdot}H_2O$ (10.0 mg, 0.05 mmol), **2** (1.5 mmol, 1.5 equiv.), **1** (1.0 mmol, 1 equiv.) and THF (5 ml) sequentially. The reaction was then carried out at room temperature under an atmosphere of air from a balloon until completion of the reaction as monitored by thin-layer chromatography. The crude reaction mixture was filtered through a short column of silica gel, eluted with ethyl acetate (4 × 5 ml) and concentrated. The residue was purified by chromatography on silica gel to afford the pure product.

Data availability

Experimental procedures, characterization of the compounds and density functional theory calculations are available in the Supplementary Information. Crystallographic data for the structures reported in this Article have been deposited at the Cambridge Crystallographic Data Centre, under deposition numbers CCDC 1939682 (*E*-**3ak**) and 1939713 (*E*-**3ed**). Copies of the data can be obtained free of charge via https://www.ccdc.cam.ac.uk/structures/. All other data are available from the corresponding authors upon reasonable request.

Received: 16 September 2020; Accepted: 26 May 2021;
Published online: 8 July 2021

References

1. Gant, T. G. Using deuterium in drug discovery: leaving the label in the drug. *J. Med. Chem.* **57**, 3595–3611 (2014).
2. Atzrodt, J., Derdau, V., Kerr, W. J. & Reid, M. Deuterium- and tritium-labelled compounds: applications in the life sciences. *Angew. Chem. Int. Ed.* **57**, 1758–1784 (2018).
3. Pirali, T., Serafini, M., Cargnin, S. & Genazzani, A. A. Applications of deuterium in medicinal chemistry. *J. Med. Chem.* **62**, 5276–5297 (2019).
4. Atzrodt, J., Derdau, V., Fey, T. & Zimmermann, J. The renaissance of H/D exchange. *Angew. Chem. Int. Ed.* **46**, 7744–7765 (2007).
5. Atzrodt, J., Derdau, V., Kerr, W. J. & Reid, M. C–H functionalisation for hydrogen isotope exchange. *Angew. Chem. Int. Ed.* **57**, 3022–3047 (2018).
6. Nguyen, T. D. et al. Isotope effect in spin response of π-conjugated polymer films and devices. *Nat. Mater.* **9**, 345–352 (2010).
7. Hirata, S., Totani, K., Watanabe, T., Kaji, H. & Vacha, M. Relationship between room temperature phosphorescence and deuteration position in a purely aromatic compound. *Chem. Phys. Lett.* **591**, 119–125 (2014).
8. Shao, M. et al. The isotopic effects of deuteration on optoelectronic properties of conducting polymers. *Nat. Commun.* **5**, 3180 (2014).
9. Bernardi, R. et al. On the components of secretion of mandibular glands of the ant *Lasius (Dendrolasius) fuliginosus*. *Tetrahedron Lett.* **8**, 3893–3896 (1967).
10. Yunker, M. B. & Scheuer, P. J. Mokupalides, three novel hexaprenoids from a marine sponge. *J. Am. Chem. Soc.* **100**, 307–309 (1978).
11. Barreiro, E. J., Kümmerle, A. E. & Fraga, C. A. M. The methylation effect in medicinal chemistry. *Chem. Rev.* **111**, 5215–5246 (2011).
12. Leung, C. S., Leung, S. S. F., Tirado-Rives, J. & Jorgensen, W. L. Methyl effects on protein–ligand binding. *J. Med. Chem.* **55**, 4489–4500 (2012).
13. Schönherr, H. & Cernak, T. Profound methyl effects in drug discovery and a call for new C–H methylation reactions. *Angew. Chem. Int. Ed.* **52**, 12256–12267 (2013).
14. Cernak, T., Dykstra, K. D., Tyagarajan, S., Vachal, P. & Krska, S. W. The medicinal chemist's toolbox for late stage functionalization of drug-like molecules. *Chem. Soc. Rev.* **45**, 546–576 (2016).
15. Young, R. J. et al. Selective and dual action orally active inhibitors of thrombin and factor Xa. *Bioorg. Med. Chem. Lett.* **17**, 2927–2930 (2007).
16. He, Z.-T., Li, H., Haydl, A. M., Whiteker, G. T. & Hartwig, J. F. Trimethylphosphate as a methylating agent for cross coupling: A slow-release mechanism for the methylation of arylboronic esters. *J. Am. Chem. Soc.* **140**, 17197–17202 (2018).
17. Feng, K. et al. Late-stage oxidative C(sp^3)–H methylation. *Nature* **580**, 621–627 (2020).
18. Friis, S. D., Johansson, M. J. & Ackermann, L. Cobalt-catalysed C–H methylation for late-stage drug diversification. *Nat. Chem.* **12**, 511–519 (2020).

19. Mullard, A. FDA approves first deuterated drug. *Nat. Rev. Drug Discov.* **16**, 305 (2017).
20. Wang, M., Zhao, Y., Zhao, Y. & Shi, Z. Bioinspired design of a robust d_3-methylating agent. *Sci. Adv.* **6**, eaba0946 (2020).
21. Hilton, M. J. et al. Investigating the nature of palladium chain-walking in the enantioselective redox-relay Heck reaction of alkenyl alcohols. *J. Org. Chem.* **79**, 11841–11850 (2014).
22. Loh, Y. Y. et al. Photoredox-catalyzed deuteration and tritiation of pharmaceutical compounds. *Science* **358**, 1182–1187 (2017).
23. Krishnakumar, V. & Gunanathan, C. Ruthenium-catalyzed selective α-deuteration of aliphatic nitriles using D_2O. *Chem. Commun.* **54**, 8705–8708 (2018).
24. Chang, Y. et al. Catalytic deuterium incorporation within metabolically stable β-amino C–H bonds of drug molecules. *J. Am. Chem. Soc.* **141**, 14570–14575 (2019).
25. Zhang, X. et al. Carbene-catalyzed α,γ-deuteration of enals under oxidative conditions. *ACS Catal.* **10**, 5475–5482 (2020).
26. Li, H. et al. Pentafluorophenyl esters: highly chemoselective ketyl precursors for the synthesis of α,α-dideuterio alcohols using SmI_2 and D_2O as a deuterium source. *Org. Lett.* **22**, 1249–1253 (2020).
27. Kurimoto, A., Sherbo, R. S., Cao, Y., Loo, N. W. X. & Berlinguette, C. P. Electrolytic deuteration of unsaturated bonds without using D_2. *Nat. Catal.* **3**, 719–726 (2020).
28. Ou, W. et al. Room-temperature palladium-catalyzed deuterogenolysis of carbon oxygen bonds towards deuterated pharmaceuticals. *Angew. Chem. Int. Ed.* **60**, 6357–6361 (2021).
29. Hartwig, J. *Organotransition Metal Chemistry: from Bonding to Catalysis* (University Science Books, 2009).
30. Tsuji, J. *Transition Metal Reagents and Catalysts: Innovations in Organic Synthesis* (Wiley, 2000).
31. Beller, M. & Bolm, C. (eds) *Transition Metals for Organic Synthesis: Building Blocks and Fine Chemicals* 2nd edn (Wiley-VCH, 2004).
32. Albada, B. & Metzler-Nolte, N. Organometallic–peptide bioconjugates: synthetic strategies and medicinal applications. *Chem. Rev.* **116**, 11797–11839 (2016).
33. Buchmeiser, M. R. Homogeneous metathesis polymerization by well-defined group VI and group VIII transition-metal alkylidenes: fundamentals and applications in the preparation of advanced materials. *Chem. Rev.* **100**, 1565–1604 (2000).
34. Yam, V. W.-W., Au, V. K.-M. & Leung, S. Y.-L. Light-emitting self-assembled materials based on d^8 and d^{10} transition metal complexes. *Chem. Rev.* **115**, 7589–7728 (2015).
35. Yamamoto, Y. & Asao, N. Selective reactions using allylic metals. *Chem. Rev.* **93**, 2207–2293 (1993).
36. Spielmann, K., Niel, G., de Figueiredo, R. M. & Campagne, J.-M. Catalytic nucleophilic 'umpoled' π-allyl reagents. *Chem. Soc. Rev.* **47**, 1159–1173 (2018).
37. Hauser, F. M., Tommasi, R., Hewawasam, P. & Rho, Y. S. Stereospecific syntheses of (*E*)-1,3-disubstituted dienes. *J. Org. Chem.* **53**, 4886–4887 (1988).
38. Wang, R., Luan, Y. & Ye, M. Transition metal-catalyzed allylic C(sp^3)–H functionalization via η^3-allylmetal intermediate. *Chin. J. Chem.* **37**, 720–743 (2019).
39. Chen, M. S., Prabagaran, N., Labenz, N. A. & White, M. C. Serial ligand catalysis: a highly selective allylic C–H oxidation. *J. Am. Chem. Soc.* **127**, 6970–6971 (2005).
40. Campbell, A. N., White, P. B., Guzei, I. A. & Stahl, S. S. Allylic C–H acetoxylation with a 4,5-diazafluorenone-ligated palladium catalyst: a ligand-based strategy to achieve aerobic catalytic turnover. *J. Am. Chem. Soc.* **132**, 15116–15119 (2010).
41. Sharma, A. & Hartwig, J. F. Enantioselective functionalization of allylic C–H bonds following a strategy of functionalization and diversification. *J. Am. Chem. Soc.* **135**, 17983–17989 (2013).
42. Li, J. et al. Site-specific allylic C–H bond functionalization with a copper-bound N-centred radical. *Nature* **574**, 516–521 (2019).
43. Andrus, M. B. & Zhou, Z. Highly enantioselective copper–bisoxazoline-catalyzed allylic oxidation of cyclic olefins with *tert*-butyl *p*-nitroperbenzoate. *J. Am. Chem. Soc.* **124**, 8806–8807 (2002).
44. Du, H., Yuan, W., Zhao, B. & Shi, Y. A Pd(0)-catalyzed diamination of terminal olefins at allylic and homoallylic carbons via formal C–H activation under solvent-free conditions. *J. Am. Chem. Soc.* **129**, 7496–7497 (2007).
45. Bayeh, L., Le, P. Q. & Tambar, U. K. Catalytic allylic oxidation of internal alkenes to a multifunctional chiral building block. *Nature* **547**, 196–200 (2017).
46. Lerchen, A. et al. Non-directed cross-dehydrogenative (hetero)arylation of allylic C(sp^3)–H bonds enabled by C–H activation. *Angew. Chem. Int. Ed.* **57**, 15248–15252 (2018).
47. Lei, H. & Rovis, T. Ir-catalyzed intermolecular branch-selective allylic C–H amidation of unactivated terminal olefins. *J. Am. Chem. Soc.* **141**, 2268–2273 (2019).
48. Zimmer, R., Dinesh, C. U., Nandanan, E. & Khan, F. A. Palladium-catalyzed reactions of allenes. *Chem. Rev.* **100**, 3067–3125 (2000).
49. Ma, S. Transition metal-catalyzed/mediated reaction of allenes with a nucleophilic functionality connected to the α-carbon atom. *Acc. Chem. Res.* **36**, 701–712 (2003).
50. Wang, W., Qian, H. & Ma, S. Rh-catalyzed reaction of propargylic alcohols with aryl boronic acids–switch from β-OH elimination to protodemetalation. *Chin. J. Chem.* **38**, 331–345 (2020).
51. Singh, J., Petter, R. C., Baillie, T. A. & Whitty, A. The resurgence of covalent drugs. *Nat. Rev. Drug Discov.* **10**, 307–317 (2011).
52. Lonsdale, R. & Ward, R. A. Structure-based design of targeted covalent inhibitors. *Chem. Soc. Rev.* **47**, 3816–3830 (2018).
53. Liu, Q. et al. Developing irreversible inhibitors of the protein kinase cysteinome. *Chem. Biol.* **20**, 146–159 (2013).
54. Huang, X. & Ma, S. Allenation of terminal alkynes with aldehydes and ketones. *Acc. Chem. Res.* **52**, 1301–1312 (2019).
55. Uma, R., Davies, M. K., Crévisy, C. & Grée, R. Efficient isomerization of allylic alcohols to saturated carbonyl compounds by activated rhodium and ruthenium complexes. *Eur. J. Org. Chem.* **2001**, 3141–3146 (2001).
56. Ahlsten, N., Lundberg, H. & Martín-Matute, B. Rhodium-catalysed isomerisation of allylic alcohols in water at ambient temperature. *Green. Chem.* **12**, 1628–1633 (2010).
57. Liu, T.-L., Ng, T. W. & Zhao, Y. Rhodium-catalyzed enantioselective isomerization of secondary allylic alcohols. *J. Am. Chem. Soc.* **139**, 3643–3646 (2017).

Acknowledgements

Financial support from the National Natural Science Foundation of China (grant numbers 21690063 and 21988101 for S.M. and grant no. 21801041 for H.Q.) is acknowledged. We thank H. Xu for reproducing the results for compounds *E*-**3am**, *E*-**3fd** and *E*-**3iv** presented in Fig. 2.

Author contributions

S.M., H.Q. and W.W. designed the experiments. W.W., Y.Y. and H.Q. performed the experiments. X.Z. and H.F. performed the density functional theory calculations. W.W., H.Q., X.Z., B.C. and S.M. wrote the manuscript.

Competing interests

The authors declare no competing interests.

Additional information

Supplementary information The online version contains supplementary material available at https://doi.org/10.1038/s41929-021-00643-9.

Correspondence and requests for materials should be addressed to X.Z., H.Q. or S.M.

Peer review information *Nature Catalysis* thanks Jie An, Yu Lan and the other, anonymous, reviewer(s) for their contribution to the peer review of this work.

Reprints and permissions information is available at www.nature.com/reprints.

Publisher's note Springer Nature remains neutral with regard to jurisdictional claims in published maps and institutional affiliations.